Adaptive Rateless Coding for Constant Bit Rate Data-Partitioned Wireless IPTV

L. Al-Jobouri, M. Fleury, and M. Ghanbari
University of Essex
School of Comp. Sci. and Elec. Eng.
Colchester, United Kingdom
{lamoha, fleum, ghan}@essex.ac.uk

Abstract— **Constant Bit-Rate (CBR) video is often preferred by broadcasters, as it allows resources to be reserved. This paper applies an adaptive channel coding scheme to CBR video. Compared to some existing schemes advantages include: the coding rate is changed according to the channel conditions; it is byte-based rather than block-based, for reduced latency; and a single retransmission allows a further attempt at reconstruction. The scheme is demonstrated on data-partitioned video, resulting in a number of trade-offs between: frame sequence structure; inclusion of intra-refresh macroblocks; and partition coding isolation. With an appropriate choice of bit-rate reasonable video quality is achieve, including for a temporally active video sequence.**

Keywords-*CBR, data-partitioning; IEEE 802.16; IPTV; mobile TV; Raptor channel coding*

I. INTRODUCTION

Application layer Forward Error Correction (AL-FEC) has been found necessary [1] for a number of error-prone wireless network environments, because of the stringent anticipated requirements for IPTV. The Digital Video Broadcast project has specified [2] optional AL rateless channel coding. Similarly, 3GPP have also adopted a rateless scheme [3]. However, neither are these schemes adapt to channel conditions but instead exploit the remarkable performance of one type of channel coding, Raptor coding [4], which has linear encode and decode computational complexity, a low error floor [5] compared to other members of the rateless coding family [6], and can be applied in systematic form. Some commercially attractive forms of IPTV, such as time-shifted TV and video-on-demand, can tolerate a request for extra redundant data, which is easily generated by a rateless coder. Content-distribution networks also reduce IPTV start-up latency to the user [7] by positioning the video serving office closer to the access network.

In this paper, an adaptive AL-FEC scheme is proposed and demonstrated for mobile IPTV over IEEE 802.16e, i.e. mobile WiMAX [8]. WiMAX is being deployed in rural areas [9] and regions that lack a 3G infrastructure. IPTV architectures for WiMAX are considered in [10] [11]. While variable bit rate video maintains constant quality and as such is of interest to researchers, constant bit rate (CBR) video is adopted by many broadcasters, as it allows prior allocation of bandwidth and storage resources. We have applied the adaptive AL-FEC scheme to a data-partitioned compressed bitstream. Data partitioning an H.264/AVC (Advanced Video Coding) codec [12] is a form of layered error resilience. As such it can provide graceful degradation of video quality and as consequently has found [13] an application in mobile video streaming. This paper caters for packets that are corrupted but may still be repairable by Raptor channel coding [4]. Prior use of application-layer Raptor coding, especially that in various standards [1], has been block-based rather than byte-based, resulting in longer repair latencies. The wireless standards also do not [1] consider channel coding rate adaptation. To achieve adaptation, channel estimation is necessary. The IEEE 802.16e standard [14] specifies that a mobile station should provide channel measurements, which can either be Received Signal Strength Indicators or may be Carrier-to-Noise-and-Interference Ratio measurements made over modulated carrier preambles.

For mobile WiMAX, capacity studies [15] suggest up to 16 mobile TV users per cell in a 'lossy' channel depending on factors such as the form of scheduling and whether MIMO antennas are activated. However, given the predicted increase in data rates arising from IEEE 802.16m, the number of unicast video users [8] with 4×2 Multi User (MU)-MIMO antennas, will be 44 at 384 kbps and 22 at 768 kbps in an urban environment. For a similar configuration but using 20 MHz rather than 80 MHz channels, the authors of [10] reported the number of unicast video users per antenna sector to be 11 and 6 depending on datarates. Notice, however, that IEEE 802.16m [16] is not backwardly compatible with IEEE 802.16e, though it does support joint operation with it.

The source coding configuration of the scheme should be considered, apart from selection of the CBR bitrate, attention should be given to the frame structure (sequence of predictively-coded P-pictures and bi-predictively coded B-pictures0; the configuration of the data-partitioning to avoid unnecessary dependencies between partitions; and to the percentage of intra-refresh (IR) macroblocks (MBs) if periodic refresh is not used, in order to avoid sudden data rate increases over constrained bandwidth. Though simulations herein select randomly IR MBs, it is possible to achieve gradual decoder

refresh [17] with IR MBs if an appropriate refresh pattern is employed.

The remainder of this paper is organized as follows. The following Section supplies background material necessary to understand Section III, which details the proposed scheme. Section IV consists of an evaluation of the scheme, while Section V concludes the paper and indicates future work.

II. BACKGOUND

This Section establishes the two components of the CBR AL-FEC scheme, namely data-partitioning and rateless coding.

A. Data-partitioning

In an H.264/AVC codec, the Network Abstraction Layer (NAL) facilitates the delivery of the Video Coding Layer (VCL) data to the underlying transportation protocols such as RTP/IP, H.32X and MPEG-2 systems. Each NAL unit (NALU) created by an H.264/AVC encoder can be considered as a packet that contains an integer number of bytes including a header and a payload. The header specifies the NALU type and the payload contains the related data. When data partitioning is enabled, every slice is divided into three separate partitions and each partition is located in either of type 2 to type-4 NALU's, as listed in Table I. A NALU of type 2, also known as partition-A, comprises the most important information of the compressed video bit stream of P- and B-pictures, that is the MB addresses, motion vectors (MV's) and essential headers. If any MB's in these pictures are intra-coded, their integer-valued Discrete Cosine Transform Transform (DCT) coefficients are packed into the type-3 NALU, also known as partition-B. Type 4 NAL, also known as partition-C, carries the DCT coefficients of the motion-compensated inter-picture coded MBs. Partitions A and B of data-partitioned P- and B-slices are small for broadcast quality video but their C-type partitions can be long when using a low Quantization Parameter (QP) (high quality video).

In order to decode partition-B and -C, the decoder must know the location from which each MB was predicted, which implies that partitions B and C cannot be reconstructed if partition-A is lost. Though partition-A is independent of partitions B and C, Constrained Intra Prediction (CIP) should be set in the codec configuration [18] to make partition-B independent of partition-C. By setting this option, partition-B MBs are no longer predicted from neighboring inter-coded MBs. This is because the prediction residuals from neighboring inter-coded MBs reside in partition-C and cannot be accessed by the decoder if a partition-C packet is lost. There is a by-product of increasing packet sizes due to a reduction in compression efficiency but the increase in size may be justified in error- prone environments.

B. Rateless channel coding

Rateless channel encoding of in the form used in this paper is accomplished as follows [6]: Choose d_i randomly from some distribution of degrees, where $\rho_{di} = Pr$[degree d_i], Pr is the probability of a given event. Choose d_i random

TABLE I. NALU TYPES

NAL unit type	Class	Content of NAL unit
0	-	Unspecified
1	VCL	Coded slice
2	VCL	Coded slice partition-A
3	VCL	Coded slice partition-B
4	VCL	Coded slice partition-C
5	VCL	Coded slice of an IDR picture
6-12	Non-VCL	Suppl. info., parameter sets, etc.
13-23	-	Reserved
24-31	-	Unspecified

information symbols R_i among k information symbols. These R_i symbols are then XORed together to produce a new composite symbol, which forms one symbol of the transmitted packet. Thus, if the symbols are bytes (as herein) then all of the R_i byte's bits are XORed with all of the bits of the other randomly selected bytes in turn. It is not necessary to specify the random degree or the random symbols chosen if it is assumed that the (pseudo-) random number generators of sender and receiver are synchronized.

Symbols are processed at the decoder as follows. If a symbol arrives with degree greater than one it is buffered. If a clean symbol arrives with degree one then it is XORed with all symbols in which it was used in the encoding process. This reduces the degree of each of the symbols to which the degree one symbol is applied. When a degree two symbol is eventually reduced to degree one, it too can be used in the decoding process. Notice that a degree one symbol for which no *XOR*ing has taken place. Notice also that for packet erasure channels a clean degree one symbol (a packet) is easily established as such.

The original degree distribution [19] (the ideal Soliton distribution) was given by:

$$\rho(1) = 1/n \tag{1}$$

$$\rho(d) = \frac{1}{d(d-1)}, \qquad d = \{2, 3, \ldots, k\} \tag{2}$$

where k is the number of source symbols. In practice, the robust Soliton distribution [6] is employed as this produces degree-one symbols at a more convenient rate for decoding. It also avoids isolated symbols that are not used elsewhere. Two tuneable parameters [6] c and δ are used to form the expected number of useable degree one symbols:

$$S = c \ln\left(\frac{k}{\delta}\right)\sqrt{k} \tag{3}$$

where c is a constant close to 1 and δ is a bound on the probability that decoding fails to complete. Then define

$$\begin{aligned} \tau(d) &= \frac{S}{k}\frac{1}{d} && \text{for } d = 1, 2, \ldots (k/S)\text{-}1 \\ &= \frac{S}{k}\ln\left(\frac{S}{\delta}\right) && \text{for } d = k/S \\ &= 0 && \text{for } d > k/S \end{aligned} \tag{4}$$

as an auxiliary positive-valued function to give the robust Soliton distribution:

$$\mu(d) = \frac{\rho(d) + \tau(d)}{z} \quad (5)$$

where z normalizes the probability distribution to unity and is given by:

$$z = \sum_{d} (\rho(d) + \tau(d)) \quad (6)$$

III. PROPOSED SCHEME

In the proposed adaptive scheme, the probability of channel byte loss (*BL*) through fast fading serves to predict the amount of redundant data to be added to the payload. The instantaneous *BL* is used to calculate the amount of redundant data adaptively added to the payload. In an implementation, *BL*, is found through measurement of channel conditions. If the original packet length is *L*, then the redundant data is given simply by

$$R = L \times BL + (L \times BL^2) + (L \times BL^3) \ldots \quad (7)$$
$$= L/(1\text{-}BL) - L,$$

which adds successively smaller additions of redundant data, based on taking the previous amount of redundant data multiplied by *BL*.

Rateless code decoding in traditional form operates by a belief-propagation algorithm [6] which is reliant upon the identification of clean symbols. This latter function is performed by PHYsical-layer forward error correction, which passes up correctly received blocks of data (through a cyclic redundancy check) but suppresses erroneous data. For example, in IEEE 802.16e, a binary, non-recursive convolutional encoder with a constraint length of 7 and a native rate of 1/2 operates at the physical layer.

The following statistical model [20]:

$$P_f(m,k) = 1 \quad \text{if } m < k,$$
$$= 0.85 \times 0.567^{m-k} \quad \text{if } m \geq k, \quad (8)$$

where is the decode failure probability of the code with k source symbols if m symbols have been successfully received (and 1 - P_f is naturally the success probability). Notice that the authors of [20] remark and show that for $k > 200$ the model almost perfectly models the performance of the code, which implies that if blocks are used approximately 200 blocks should be received before reasonable behavior takes place. This observation motivated the choice of bytes within a packet as the symbols, to reduce latencies. Upon receipt of the correctly received data, decoding of the information symbols is attempted, which will fail with a probability given by (8) for $k > 200$.

If a packet cannot be decoded, despite the provision of redundant data then extra redundant data are added to the next packet. In Fig. 1, packet X is corrupted to such an extent that it cannot be immediately decoded. Therefore, in packet X+1 some extra redundant data are included up to the level that its

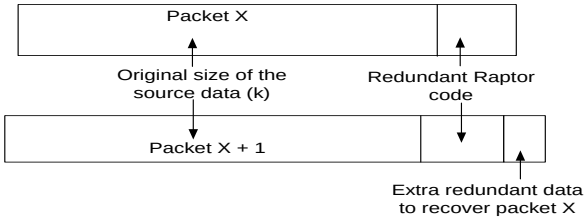

Fig.1. Division of payload data in a packet between source data, original redundant data and piggybacked data for a previous erroneous packet

decode failure is no longer certain. If according to (8), $m < k$ then a packet is corrupted to such an extent that it is effectively dropped. However, this was found in simulations to be a rare event.

It is implied from (8) that if less than k symbols (bytes) in the payload are successfully received then a further $k - m + e$ redundant bytes can be sent to reduce the risk of failure. This reduced risk arises because of the exponential decay of the risk that is evident from equation (8) and which gives rise to Raptor code's low error probability floor [5].

IV. EVALUATION

This Section describes the simulation model employed and the resulting findings.

A. Simulation model

In the proposed adaptive scheme, the probability of channel byte loss (*BL*) through fast fading in the Gilbert-Elliott channel model [21] served to predict the amount of redundant data to be added to the payload. There are two hidden states (good and bad) in this two-state Markov model. If P_{GB} and P_{BG} are the probabilities of going from good to bad state and from going from bad to good state respectively, then

$$\pi_G = P_{BG}/(P_{BG} + P_{GB}) \quad (9)$$
$$\pi_B = P_{GB}/(P_{BG} + P_{GB}) \quad (10)$$

are the steady state probabilities of being in the good and bad states. P_G and P_B are the probabilities of (byte) loss in the good and bad states respectively. Both states were modelled by a Uniform distribution. Consequently, the mean probability of channel byte loss is given by

$$BL_{mean} = P_G . \pi_G + P_B . \pi_B \quad (11)$$

which was the mean of a Uniform distribution. Thus, in simulations *BL* was selected from a Uniform distribution with mean BL_{mean}.

Assuming perfect channel knowledge of the channel conditions when the original packet was transmitted establishes an upper bound beyond which the performance of the adaptive scheme cannot improve. However, we have included measurement noise into the estimate of *BL* to test the robustness of the scheme. Measurement noise was modelled as a zero-mean Gaussian (normal) distribution and added up to a given percentage ($\pm$ 5% in the evaluation) to the packet loss probability estimate.

In simulations, the decision on whether the Raptor code belief propagation algorithm would run to completion was taken by comparing a Uniformly-distributed random variable's value with that of the probability given by (9). In the tests, *e* was set to four, resulting in a risk of failure (from (9)) of 8.7 % in reconstructing the original packet, if the extra redundant data successfully arrives.

The tests were performed on both the reference *Football* (high temporal coding complexity) and *Paris* (limited motion and higher spatial coding complexity) video sequences encoded in Common Intermediate Format (CIF) @ 30 Hz. The frame structure was IPPP…, i.e. one initial I-picture and all P, *or* IBBPBBP…, i.e. insertion of bi-predictive B-pictures for greater coding efficiency. By default, 2% IR MB's were randomly inserted. As *Football* is 9s in duration at 30 frame/s, *Paris*, a longer sequence, was reduced to 10s for comparison purposes.

The video stream was transmitted to an IEEE 802.16e mobile station (MS) and, to introduce sources of traffic congestion, a permanently available FTP source was introduced with TCP transport to a second MS. Likewise, a CBR source with packet size of 1000 B (the WiMAX maximum transfer unit) and inter-packet gap of 30 ms was also downloaded to a third MS.

The simulations adopted the mandatory settings for a 10.67 Mbps downlink (DL) rate with 3:1 DL/UL sub-frame ratio for the only WiMAX forum frame size [8] of 5 ms, 16-QAM ½ modulation over a 10 MHz channel with IEEE 802.16e recommended antenna heights and transmit/receive powers. MS's were within one km of a WiMAX base station. A WiMAX packet in the simulations is a single MAC Service Data Unit encapsulated in a MAC Protocol Data Unit. Buffers were set to 50 WiMAX packets, as larger buffers would incur delays for real-time streaming and would be inappropriate for mobile devices.

In the Gilbert-Elliott model for the ns-2 simulator, the settings for fast fading were P_{GG} (probability of being in a good state) was set to 0.95, P_{BB} (probability of being in a bad state) = 0.96, P_G = 0.02 and P_B = 0.165. The Gilbert-Elliott scheme though simple has been widely adopted, as it is thought to realistically model the burst errors that do occur and, more significantly, can be particularly damaging to compressed video streams, because of the predictive nature of source coding. Therefore, the impact of 'bursty' errors [22] should be assessed in video streaming applications.

Data points are the mean of ten independent runs, with time allowed for the simulator to reach steady state. The IEEE 802.16e add-on from the Change Gung University, Taiwan [23] was employed.

B. Findings

The data-partitioned video streams under the default configuration (2% IR MB's, with CIP set, and a frame structure of IPPP…) were streamed from the WiMAX BS to the MS at two different rates. As might be expected in Fig. 2 the percentages of packets dropped (through buffer overflow and/or outright packet drops — m < k in (2)) is higher for the higher data-rate. Surprisingly given its greater temporal complexity, *Football* suffered a smaller percentage of packet drops at 500 kbps though the difference to *Paris* is small. For the same bit-rate, *Football* compared to *Paris* generally will have a higher QP, lower quality, and relatively larger partition-A packets. The type of frame structure makes little difference to the number of packets dropped in Fig. 3. However, turning off CIP does alter the packet drop numbers. Turning off CIP increases the proportion of the bitrate allocated to partition-B. Increasing the percentage of IR MBs also leads to larger partition-B carrying packets and consequently there are more packet drops. Thus in general, configuration changes that cause a relative growth in the size of packets bearing partitions -A and –B cause an increase in packet drops.

Figs. 4 and 5 examine objective video quality. In Fig. 5, despite the higher drop rates at the higher data rates reduces video quality. The impact of temporal coding complexity is observed in the lower PSNR for *Football* at 1 Mbp; it is harder to reconstruct at the decoder. From Fig. 6, choice of an IBBP… frame structure results in a drop in quality, indicating that the compression efficiency gained by including B-pictures may not be advisable. If B-pictures are coded then P-pictures becomes larger because of the greater reference distance. Consequently, loss of the now more important P-picture packets has more of an impact. In fact, B-pictures are not included in the Baseline profile of H.264/AVC, because of their coding complexity. Not including CIP, despite the lower packet drops, also weakens the video quality because of the difficulty of reconstructing with partition-C if partition-B is missing. Finally, the gain from including more IR MB's (5% compared to 2%) does not outweigh the risk of loss of larger partition-B packets.

Corrupted packets are generally repaired by the adaptive coding scheme, as otherwise the percentages of packets

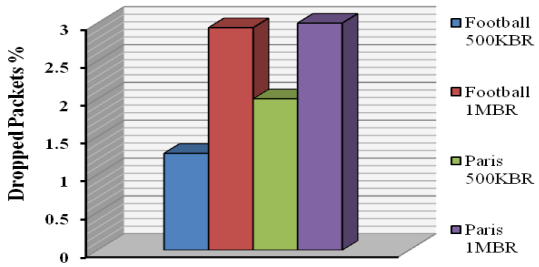

Fig. 2 Percentage dropped packets for CBR streaming with different target bitrates and content with 2% IR MBs with CIP.

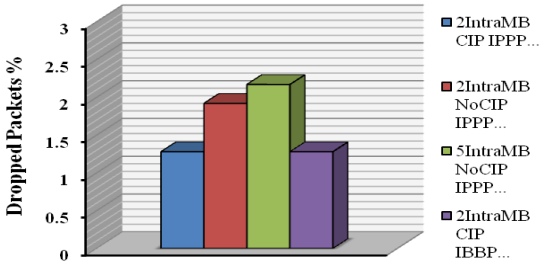

Fig. 3. Percentage dropped packets for CBR streaming with a variety of configurations for *Football* at 500 kbps.

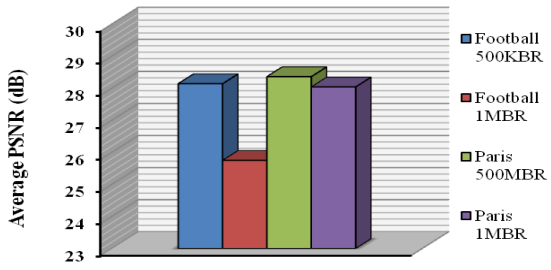

Fig. 4. Average video quality (Y-PSNR) for CBR streaming with different target bitrates and content with 2% IR MBs with CIP.

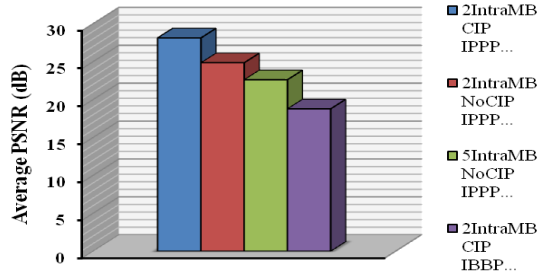

Fig. 5. Average video quality (Y-PSNR) for CBR streaming with a variety of configurations for *Football* at 500 kbps.

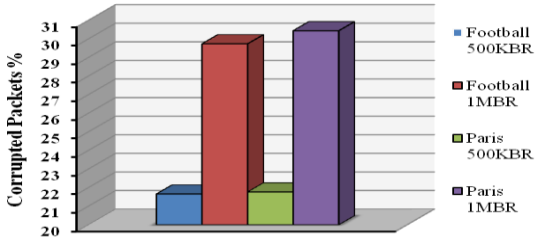

Fig. 6. Percentage corrupted packets for CBR streaming with different target bitrates and content with 2% IR MBs with CIP.

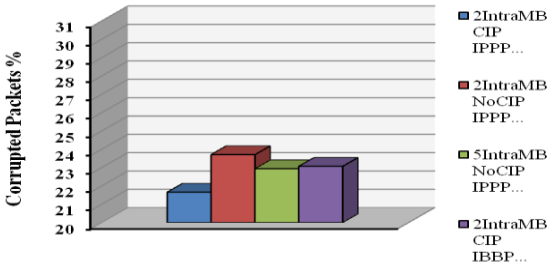

Fig. 7. Percentage of corrupted packets for CBR streaming with a variety of configurations for *Football* at 500 kbps.

affected in Figs. 6 and 7 would be overwhelming. Predictably, the larger packets at the higher bit-rate are more impacted by channel conditions. A setting of 2% IR MB's with CIP set results in the least corrupted packets. The main impact of an increased number of corrupted packets is an increase in the total delay experienced. For uncorrupted packets, the mean end-to-end delay across all schemes is between 7 and 9 ms. Due to the retransmission of extra redundant data, this rise to between 17 and 18 ms. Thus, at the higher data rate there is a significant additional delay.

From these findings, with the adaptive channel coding scheme it is possible to achieve 'fair' video quality of around 28 dB at a CBR rate of 500 kbps. This requires tuning of the configuration to use an IPPP… frame structure with CIP set and 2% IR MB's.

V. CONCLUSION

We have proposed an AL-FEC scheme which adapts to channel conditions and which provides extra redundant data if initial reconstruction fails. Provided packet sizes are not too large then the delay caused by the single retransmission after a request over the next WiMAX sub-frame is reduced. As data-partitioning is used it was found important to tune the video configuration with a small percentage of intra-refresh macroblocks, independent partition-B and partition-Cs (as this is not guaranteed) and a frame structure that avoids B-pictures. In the 'bursty' channel conditions simulated, 'fair' video quality (over 25 dB) is more likely than 'good' quality (over 31 dB). Packet drops were below 5% in the experiments, which was convenient as AL-FEC has no remedy for packets that fail to arrive. Data-partitioning can reduce the effect of packet loss by assigning more important source coding data to smaller packets. However, it is also possible that duplicate partition-A and partition-B carrying packets should be sent in severe channel conditions, as future work will investigate.

REFERENCES

[1] M. Luby, T. Stockhammer, and M. Watson, "Application layer FEC in IPTV services," *IEEE Commun. Mag.*, vol. 46, no. 5, pp. 95-101, 2008.

[2] ETSI TS 102 034 v1.3.1, "Transport of MPEG 2 Transport Stream (TS) Based DVB Services over IP Based Networks," DVB Blue Book A086rev5, http://www.dvb.org/technology/bluebooks, Oct. 2007.

[3] 3GPP TS26.346, "Multimedia Broadcast/Multicast Service (MBMS): Protocols and Codecs," Dec. 2005.

[4] A. Shokorallahi, "Raptor codes," *IEEE Trans. Info. Theory*, vol. 52, no. 6, pp. 2551-2567, 2006.

[5] R. Palanki, and J. Yedidai, "Rateless codes on noisy channels." in *Int. Symp. Info. Theory*, 2004, p. 37.

[6] D.J.C. MacKay "Fountain codes*," IEE Proc.: Commun.*, vol. 152, no. 6, pp. 1062–1068, 2005.

[7] N. Degrande, K. Laevens, and D. De Vleeschauwer, "Increasing the user perceived quality for IPTV services," *IEEE Commun. Mag.*, vol. 46, no. 2, pp. 94–100, 2008.

[8] R. Jain, C. So-In, and A.-K Al-Tamimi, "System-level modeling of IEEE 802.16e mobile WiMAX networks," *IEEE Wireless Commun.*, vol. 15, no. 5, pp. 73–79, 2008.

[9] O. Hillested, A. Perkis, V. Genc, S. Murphy, and L. Murphy, "Delivery of on-demand video services in rural areas via IEEE 802.16 broadband wireless access networks," in *Proc. of 2nd Int'l Workshop on Wireless Multimedia Networking and Performance Modeling*, 2006, pp. 43-52.

[10] O. Oyman, J. Foerster, Y.-j. Tcha, and S.-C. Lee, "Towards enhanced mobile video services over WiMAX and LTE," *IEEE Commun. Mag.*, vol. 48, no. 8, pp. 68–76, 2010.

[11] I.V. Uilecan, C. Zhou, and G.E. Atkin, "Framework for delivering IPTV services over WiMAX wireless networks," in *Proc. of IEEE Int'l Conf. on Elec./Info. Technol.*, 2007, pp. 470–475.

[12] S. Wenger, "H.264/AVC over IP," *IEEE Trans. Circuits Syst. Video Technol.*, vol. 13, no. 7, pp. 645-655, 2003.

[13] T. Stockhammer, and M. Bystrom, "H.264/AVC data partitioning for mobile video communication," in *IEEE Int'l Conf. on Image Processing*, 2004, pp. 545-548.

[14] IEEE, 802.16e-2005. "IEEE standard for local and metropolitan Area networks. Part 16: Air interface for fixed and mobile broadband wireless access systems," 2005.

[15] C. So-In, R. Jain, A.-K. Tamimi, "Capacity Evaluation for IEEE 802.16e mobile WiMAX," *J. of Comp. Syst., Networks, and Commun*., [online journal] 12 pages, 2010.

[16] S. Ahmadi, *Mobile WiMAX: A systems approach to understanding IEEE 802.16m radio access technology*, Academic Press, Amsterdam, 2011.

[17] M.M. Hannuksela, Y.-K. Wang, and M. Gabbouj, "Random access using isolated areas," in *Proc. of IEEE Int'l Conf. on Image Process.*, 2003, pp. 841-844.

[18] Y. Dhondt, S. Mys, K. Vermeirsch, and R. Van de Walle, "Constrained inter prediction: Removing dependencies between different data partitions," in *Proc. of Advanced Concepts for Intelligent Visual Systems*, 2007, pp. 720-731.

[19] M. Luby "LT codes," in *Proc. of 34rd Ann. IEEE Symp. on Foundations of Computer Science*, 2002, pp. 271–280.

[20] M. Luby, T. Gasiba, T. Stockhammer, and M. Watson, "Reliable multimedia download delivery in cellular broadcast networks," *IEEE Trans. Broadcast.*, vol. 53, no. 1, pp. 235-246, 2007.

[21] G. Haßlinger, and O. Hohlfeld, "The Gilbert-Elliott model for packet loss in real time services on the Internet," in *14th GI/ITG Conf. on Measurement, Modelling, and Evaluation of Computer and Commun. Systs.*, 2008, pp. 269-283.

[22] J. Liang, J.G. Apostolopoulos, and B. Girod, "Analysis of packet loss for compressed video: Effect of burst losses and correlation between error frames," *IEEE Trans. Circ. Syst. Video Technol.*, vol. 18, no. 7, pp. 861-874, 2008.

[23] F.C.D. Tsai, et al., "The design and implementation of WiMAX module for ns-2 simulator," *Workshop on ns2: the IP network simulator*, 2006, article no. 5.